Evaluation of the absolute single-photon detection efficiency of HRPPD

Yifan Jin[1], Alexander Kiselev[1] and Sean Stoll[1]

[1] Physics Department, Brookhaven National Laboratory

Abstract :

Pixelated High Rate Picosecond Photon Detectors (HRPPDs) by Incom Inc. are promising photosensors for use in Ring Imaging CHerenkov (RICH) detectors, where a high gain, sub-mm position resolution and sub-100ps timing resolution are required in a single photon mode. Quantum Efficiency (QE) has been measured for the first batch of EIC HRPPDs both by Incom and EIC research groups at Jefferson Lab and Brookhaven Lab, with peak values at ~365 nm typically exceeding 30%. In this study, we present a first direct measurement of HRPPD Photon Detection Efficiency (PDE) being equal to 19.3 ± 0.2 (stat) ± 0.8 (sys) % at 398.6 nm, in a photoelectron pulse counting mode using a picosecond diode laser. HRPPD QE at the same spot and at the same wavelength was evaluated to be 24.3 ± 0.1 (stat) ± 0.5 (sys) %, leading to a Collection Efficiency (CE) estimate of ~79%, which is consistent with the expectations.

Index Terms: HRPPD, photon detection efficiency.

1 Methodology

To measure the PDE, we used picosecond diode laser light pulses in a configuration shown in Figure 1 (left).

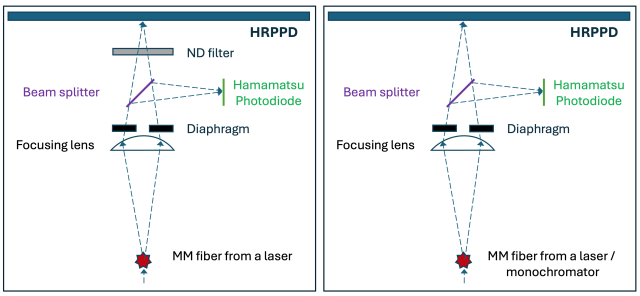

Figure 1. A schematic view of our PDE measurement setup (left) and a QE measurement setup (right).

The laser beam was split into two paths: direct light focused onto the HRPPD photocathode, at a location matching the center of one of the anode pads (pixels), and light reflected at 90 degrees impinging on a reference photodiode. While a high photon flux is desirable for accurate current monitoring by this photodiode, a much reduced photon flux is required for the HRPPD to ensure a low photon counting mode. To resolve this discrepancy, a neutral density (ND) filter was placed between the beam splitter and the HRPPD.

Assume that the number of photons incident on the HRPPD in a single laser pulse follows a Poisson distribution with a mean λ, and that each photon is detected independently with a probability p, corresponding to the PDE. Then, the probability that the HRPPD does not detect any signal from a given pulse is:

$$P(\text{no signal}) = \sum_{n=0}^{\infty} P(n)(1-p)^n, \tag{1}$$

where $P(n) = \frac{\lambda^n e^{-\lambda}}{n!}$.

$$P(\text{no signal}) = \sum_{n=0}^{\infty} \frac{(\lambda(1-p))^n e^{-\lambda}}{n!} = e^{\lambda(1-p)} \times e^{-\lambda} = e^{-\lambda p} \tag{2}$$

$$p = \frac{ln(P(\text{no signal}))}{-\lambda} \tag{3}$$

Note that the mean photon number λ does not need to be small for this expression to hold. In other words, operation in a single-photon mode is not necessary for this method.

The mean number of photons in a single laser pulse (λ) incident on HRPPD can be derived from the following expression: $\lambda = \frac{I \cdot R}{e \cdot QE \cdot f \cdot A}$, where I is the current as measured by the reference Hamamatsu photodiode (see Figure 1), QE is its quantum efficiency at the laser wavelength, R is a ratio of the transmitted and the reflected light after the beam splitter at this wavelength, e is the elementary charge, f is a laser repetition rate, and A is an attenuation factor of the ND filter.

Since neither the beam splitter ratio R nor QE of the reference photodiode is known precisely enough, the R/QE ratio was measured by a Newport NIST traceable photodiode installed in place of an HRPPD, as explained in detail in Section 3. The attenuation factor A of the ND filter was also measured separately. Once the R/QE ratio and the A factor are calibrated, Formula 3 gives a PDE estimate.

We also evaluated a QE at the same HRPPD active area spot, by measuring a photocurrent at the same photocathode voltage (see Figure 1 right), and extracted the Collection Efficiency (CE) as a PDE/QE ratio.

It is worth noting that the photon detection efficiency (PDE) is typically determined using a different method (Lehmann et al., 2024). In that approach, the pulse amplitude at the anode is measured and then divided by the gain, obtained from a spectral fit, to estimate the number of photoelectrons generated after the photocathode. In contrast, we count signal pulses in a binary manner, thereby eliminating the dependence on gain.

2 Experimental setup

A newly established HRPPD aging test stand at Brookhaven National Laboratory (see Figure 2) was used to perform the measurements. The whole set of essential equipment, together with the typical settings, is listed below.

2.1 HRPPD and readout backplane

We used HRPPD #16 (serial number assigned by InCom Inc.) for these measurements. It was mounted on a side wall of the dark box used for aging studies, as shown in Figure 3. The HRPPD was

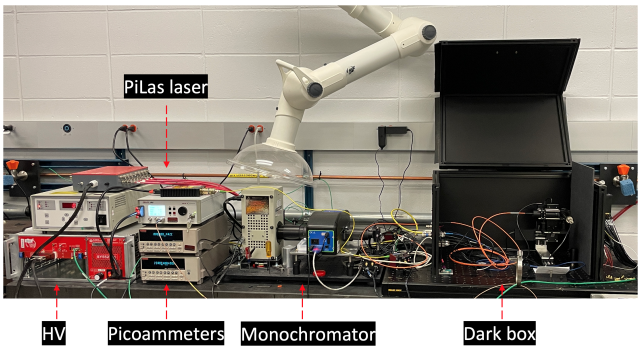

Figure 2. Experimental setup.

equipped with a Q02c passive readout backplane and a pair of 32-channel M02c MCX adapters, which allowed us to fully instrument a single 8x8 anode pad spot.

Pads of the other fifteen 8x8 pad spots were terminated to ground via 50-ohm resistors using S02c plugin cards.

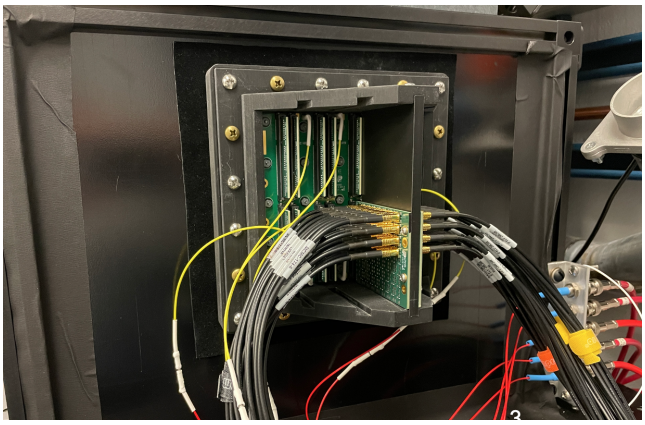

Figure 3. HRPPD #16 mounted on a dark box side wall. One can also see the interface board with a pair of plugin MCX adapters.

2.2 Dark box equipment

An optical setup shown schematically in Figure 1 was mounted on an XYZ motion control system (three Thorlabs MTS50/M translation stages) as shown in the same orientation in Figure 4.

A UV-resilient UM22-600 multi-mode fiber with a core diameter of 600 μm by Thorlabs was used between the dark box patch panel and the optical head for both PDE and QE, as well as for the calibration measurements. The light was focused by a LA1422 N-BK7 plano-convex lens with a focal distance of 40 mm, with its intensity and angular spread limited by a SM1D12C diaphragm with a chosen ~3.5 mm diameter setting, and split into two paths by a CM1-BP145B5 pellicle beam splitter, all by Thorlabs.

Light reflected at 90 degrees was detected by a Hamamatsu S1226-8BQ reference photodiode installed in a custom support inside a 1" diameter tube, at a distance roughly the same as the distance between the beam splitter and the HRPPD window.

Light passing through was detected by either an HRPPD during the measurements (as shown in the picture) or by a NIST traceable Newport 818-UV-DB photodiode for calibration purposes. According to the factory test report, the photodiode responsivity was equal to {1.6864E-1 A/W at 390 nm and 1.7957E-1 A/W at 400 nm} in a configuration without an external OD3 filter and {4.0227E-4 A/W at 390 nm and 4.2081E-4 A/W at 400 nm} with the filter installed. The uncertainty of this calibration is supposed to be 1.65% at the wavelength of interest (398.6 nm, see section 2.4 below). After a simple linear interpolation, conversion to quantum efficiency units, and error propagation, we obtain a QE of the Newport photodiode at 398.6 nm to be equal to 55.4 ± 0.9 %, and the attenuation factor of the factory OD3 filter at this wavelength equal to 426 ± 10.

None of the elements shown in Figure 4 was either changed or moved between PDE and QE measurements. In particular, we used the same fiber, diaphragm diameter setting, and XYZ-coordinates of the optical head. For calibration, either an ND filter or a Newport photodiode was mounted downstream of the beam splitter as explained in the subsequent sections.

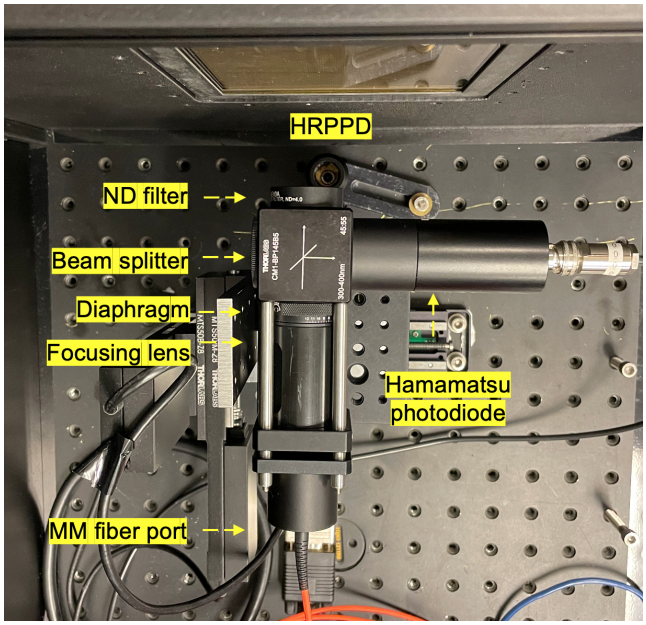

Figure 4. A small breadboard with focusing optics mounted on a 3D motion control system inside the dark box. The incoming laser beam, after passing through a beam splitter, was partly focused on the HRPPD photocathode, and partly detected by a reference photodiode. See text for more details.

2.3 High Voltage

For the PDE measurements, the HRPPD was biased using a stackable CAEN A1515BV high voltage power supply in a SY5527LC mainframe. We used the following settings: MCP bias 650 V, photocathode and transfer voltages: 200 V (gain around 4×10^6 for a particular illuminated pixel, see also a blue dashed line in Figure 10).

For the QE measurements, a 200 V bias was provided by the same Keithley 6487 picoammeter used to measure the photocurrent. Other HRPPD electrodes were floating in this case.

2.4 Laser

An NKT Photonics picosecond laser with a PiL1-040-40FC head was used for both the PDE (in a photoelectron pulse counting mode) and the QE (in a photocathode current measurement mode) evaluation. According to its test report, the laser produced light with a wavelength of 398.6 nm. This value is used in all of our estimates. Laser light was coupled into a single-mode fiber with a nominal core diameter of 3 μm, and then into a 600 μm diameter multi-mode fiber inside of the dark box.

2.5 Monochromator

A Newport MKS CS130B-1-FH monochromator with a 150 W 66477-150XV-R1 Xenon arc lamp was used for complementary QE measurements in the same setup, to observe a possible difference between a pulsed and a continuous light sources. The monochromator grating grid setting was tuned in such a way that its average wavelength as measured by a spectrometer (see Section 2.6) was the same as for the laser.

2.6 Spectrometer

A compact SR-6UVV240-25 fiber spectrometer by Ocean Optics was used to measure the actual laser and monochromator wavelengths, as shown in Figure 5.

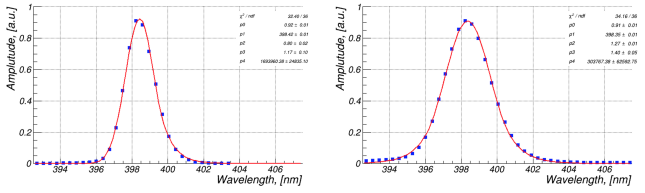

Figure 5. Left: PiLas laser wavelength spectrum with a peak value of ~398.4 nm and FWHM ~1.9 nm as measured by the Ocean Optics spectrometer. Right: Newport monochromator wavelength spectrum with a FWHM ~3.0 nm and a peak value matching the laser one within 0.1 nm as measured by the same spectrometer when using a monochromator wavelength setting of 395.7 nm .

We did not observe any noticeable shift in the laser wavelength in the range of repetition rates between 1 kHz and 40 MHz at either a 0% or a 60% tune, as well as in a range of tunes between 0% and 60% at a fixed repetition rate of 500 kHz, although the FWHM was getting up to ~10% bigger at higher tune values.

As follows from Figure 5 (left), a measured PiLas laser wavelength of ~398.4 nm matched very well 398.6 nm provided in the factory report. However, the monochromator scale was found to be off by almost 3 nm. In the complementary QE measurements described in Section 5, we therefore used a slightly different setting of 395.7 nm in the monochromator steering script, in order to perfectly match the wavelength spectra peak values between the PiLas laser and the monochromator, as seen in Figure 5.

2.7 Picoammeters

A Keithley 6485 unit was used to measure photocurrent of the Hamamatsu reference photodiode. A Keithley 6487 was used for the NIST traceable Newport photodiode as well as the HRPPD. For correlated measurements between a pair of picoammeters (see Section 3 below) their measurement ranges have always been fixed to a value matching the largest measured current, and the AUTO range setting feature turned off.

2.8 Beam spot imaging

We used an AmScope MD310C-BS bare sensor CMOS camera with a 5.12 mm x 3.84 mm sensor (2.5 μm pixels), installed at a location of the HRPPD window to air boundary, to verify a focused beam spot size. Obtained images for both the laser and the monochromator light sources are shown in Figure 6. As seen from this figure, beam diameter in both cases was about 1.0 mm (mostly defined by the fiber diameter of 600 μm), though the monochromator image looks like a "more smooth" disc. A beam spot of this size was indeed well within the 8 mm x 8 mm active area of the Hamamatsu reference photodiode.

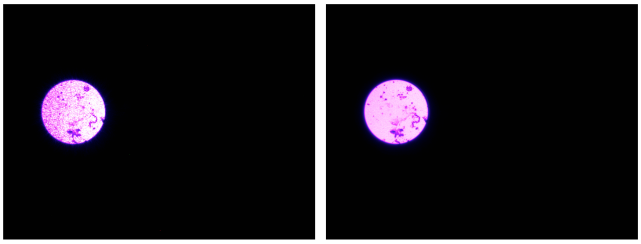

Figure 6. Left: PiLas laser beam spot image at the HRPPD window to air boundary location. Right: Newport monochromator beam image in the same optical configuration (fiber type, lens location, diaphragm opening).

2.9 DAQ, readout electronics, steering software

Software used to steer all of the setup components, as well as the RCDAQ data acquisition system was installed on a Debian 12 desktop PC. Python scripts to operate the monochromator, picoammeters, and translation stages, were written from scratch. Trigger logic was assembled in a NIM crate, while a pair of CAEN V1742 digitizers in a VME crate was operated via respective CAENET optical links by RCDAQ via a PCIe A3818 interface card.

3 Reference photodiode and ND filter calibration

The reference Hamamatsu photodiode does not come with a reliable factory calibration. Besides this, as it was mentioned earlier, neither the beam splitter ratio nor the ND filter optical density *at a laser wavelength* is known with a sufficient accuracy. In order to relate a reference Hamamatsu photodiode current to a NIST traceable Newport photodiode one, in a configuration with a beam splitter and (optionally) an ND filter installed downstream of it, we performed a series of measurements in configurations shown schematically in Figure 7. We considered three cases: (1) no filter installed between the beam splitter and the Newport photodiode, (2) a nominally OD3 reflective filter installed which came together with the Newport photodiode (see Section 2.2), (3) a nominally OD4 absorptive Thorlabs filter we were eventually using to perform the PDE measurements.

Results are presented in Figure 8. The PiLas Laser was set at a 0% tune (maximum pulse intensity). Average integrated light intensity was varied by changing a laser repetition rate between 30 kHz and 40 MHz in roughly half a decade steps (10 points on a "no filter" curve in Figure 8). Ten current measurements per point were taken, and their average and standard deviation are used in

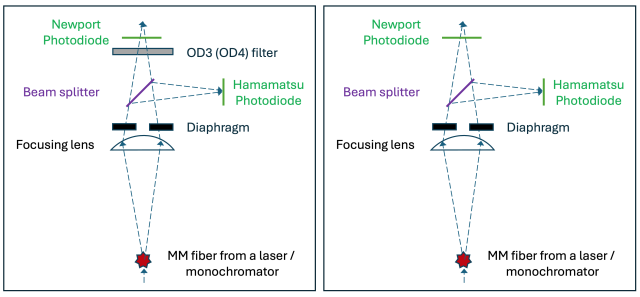

Figure 7. Configurations used to cross-calibrate Newport and Hamamatsu photodiodes, as well as our OD4 neutral density filter.

three separate $f(x) = ax+b$ straight line fits. In all three cases, we observed a perfect linearity within the measurement errors (χ^2 of 5.4, 5.2, and 0.02 per 8, 6, and 2 degrees of freedom, respectively), and b-terms consistent with 0.

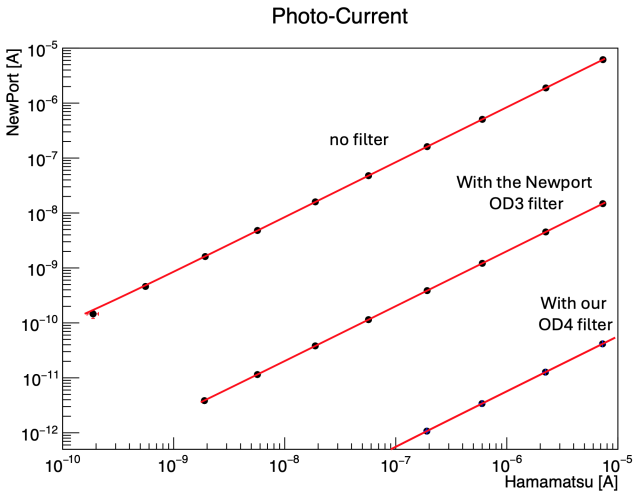

Figure 8. Currents measured by the Newport and Hamamatsu photodiodes at various PiLas laser intensities, for the configurations shown in Figure 7.

We used this evidence as an indirect proof that (1) Hamamatsu photodiode has a linear response over four decades in light intensity, (2) one can safely use a slope of the "no filter" straight line in Figure 8 to calibrate the Hamamatsu reference photodiode against the Newport one *for QE measurements*, (3) in a similar way, one can use a ratio of the "Our OD4 filter" and "no filter" line slopes in Figure 8 to cross-calibrate the Hamamatsu photodiode in a low light intensity configuration required *to measure the HRPPD PDE in a photoelectron counting mode*. Numerically, the slope of the "no filter" straight line was found equal to 0.8409 ± 0.0003, and the ratio of the "no filter" and "Our OD4 filter" slopes (effectively the optical density of our OD4 filter at 398.6 nm) was equal to 147420 ± 90.

It is worth mentioning that the "Newport OD3 filter" data were taken with a neutral density filter, for which a separate factory calibration was provided (see Section 2.2). Our measured slope ratio of the "Newport OD3 filter" and "no filter" curves came out equal to 416.9 ± 0.2, consistent with these factory calibrations at 398.6 nm within the quoted errors.

4 HRPPD PDE measurement

The measurement was performed in a configuration shown schematically in Figure 1, with our nominally OD4 neutral density filter installed between the beam splitter and the HRPPD window. The PiLas laser was run with a repetition rate of 1 kHz at a set of tunes listed in Table 1. RCDAQ DAQ was used to take the waveform data of all the 8x8 pads around the illuminated spot. V1742 digitizers were running at a 5 GS/s sampling rate. Trigger for the DAQ was provided by the PiLas laser itself. A panel of a typical "event" is shown in Figure 9, where a horizontal range is 40 ns and a vertical range is 50 mV in each of the waveforms of the 3x3 pads surrounding the illuminated one.

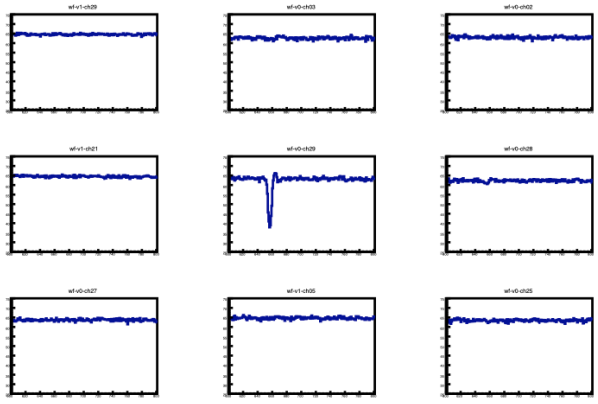

Figure 9. A single event with waveforms of the 3x3 HRPPD pad signals around the illuminated one.

Despite the fact that a majority of recorded events looked like in Figure 9 (only the illuminated pad had a measurable signal), we also considered various summation schemes for a 3x3 pad area around the illuminated spot. At the end, we decided to use waveforms of the illuminated pad and four neighboring pads for the collected charge measurements. No peak search algorithm was used. HRPPD signal was taken as a sum of 16 waveform samples (a 3.2 ns wide window) at a fixed timing offset with respect to a digitized trigger pulse. The baseline was estimated on an event-per-event basis in a same width (3.2 ns) window just in front of the location of the expected HRPPD peak, in the same waveform. Collected charge was calculated as a difference between the "peak" value (a sum over 16 samples as explained earlier, whether there was a measurable peak observed or not) and a baseline. Charge distribution, normalized to a detected electron count (which in a pure single photon mode would effectively have a meaning of the HRPPD gain) is shown in Figure 10, together with a Gaussian fit to a pedestal peak (events where HRPPD did not produce a measurable signal) and a two-Gaussian fit to the actual signal distribution, assuming that three-photoelectron event probability was small and therefore irrelevant.

One can see that the HRPPD was operated at a gain of about 4×10^6. The pedestal peak had $\sigma \sim 0.09 \times 10^6$. A fraction of events with a measurable HRPPD signal required in formula 3 was determined as a ratio of events with a collected charge above 3σ with respect to the pedestal mean, and the total number of triggers.

Since the Hamamatsu reference photodiode current was recorded at the same time, both in LASER ON and LASER OFF

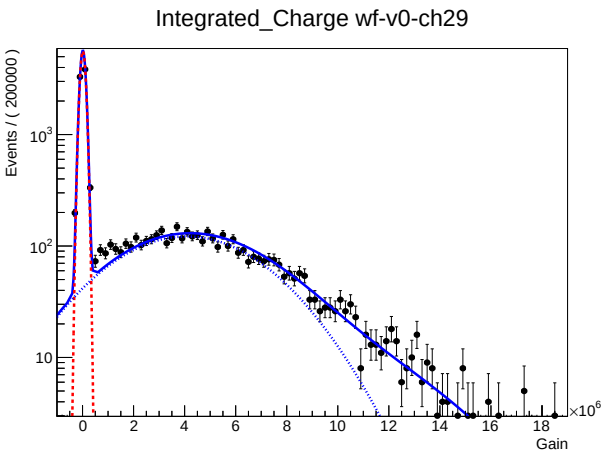

Figure 10. Charge collected by the illuminated HRPPD pad. Red dashed line indicates the fit to the pedestal, blue dashed line the one-photon peak. Blue solid line is the sum of the fits to one-photon peak and two-photon peak.

configurations , an average number of photons impinging onto the HRPPD photocathode per laser pulse was known precisely. Substituting the numbers into formula 3, and propagating the statistical errors, one obtains the PDE values.

We repeated the same measurements at a set of different laser tunes corresponding to a substantially different average fraction of non-empty events, and obtained consistent PDE values, all listed in Table 1. A statistical average of 19.3 ± 0.2 ($\chi^2 \sim 2.2$ for 2 degrees of freedom) is taken as a final result.

tune	λ	events above threshold	PDE
36.0%	4.978 ± 0.010	61.4 ± 0.4%	18.9 ± 0.2%
46.0%	3.713 ± 0.007	51.7 ± 0.5%	19.4 ± 0.3%
52.4%	2.573 ± 0.013	39.8 ± 0.4%	19.5 ± 0.3%

Table 1
Results of three sets of data using different laser tunes, listed in the first column. The second column (λ) is the mean number of photons impinging on the HRPPD photocathode per laser pulse. Only statistical errors are quoted.

4.1 Statistical and systematic uncertainties

Statistical uncertainties quoted in Table 1 follow from fit errors of the photodiode calibration curves (see Section 3), spread of the reference photodiode current measurements, binomial error when calculating a fraction of events with HRPPD pulses above threshold, as well as its error propagation in formula 3.

We assign a systematic uncertainty of 0.8% to this PDE estimate, reflecting measured quantity fluctuations during a setting up stage when the components were mounted and dismounted a number of times before the final data set was taken, effect of a threshold variation when calculating number of HRPPD pulses, as well as a 1.65% relative uncertainty of the Newport photodiode calibration.

5 HRPPD QE measurement

We performed the QE measurement using both the PiLas laser (at a variety of tunes and repetition rates) and the monochromator, in order to see a possible difference between a pulsed and a continuous light source. A configuration shown in Figure 1 (right) was used in both cases, without changing anything inside of the dark box. The photocathode bias voltage was 200 V, provided by the Keithley 6487 picoammeter. The results are listed in Table 2. The light source was turned off for about ten minutes between the successive measurements, which were taken in a sequence as listed in the table.

light source	HRPPD PC current	QE
PiLas laser @ 40 MHz, tune 0%	~2006 nA	23.1 ± 0.3 %
PiLas laser @ 30 MHz, tune 0%	~1575 nA	22.7 ± 0.3 %
PiLas laser @ 20 MHz, tune 0%	~1173 nA	22.9 ± 0.3 %
PiLas laser @ 10 MHz, tune 0%	~625 nA	23.3 ± 0.2 %
PiLas laser @ 1 MHz, tune 0%	~56 nA	24.3 ± 0.1 %
PiLas laser @ 40 MHz, tune 0%	~1916 nA	22.0 ± 0.4 %
PiLas laser @ 40 MHz, tune 60%	~957 nA	22.7 ± 0.3 %
PiLas laser @ 40 MHz, tune 80%	~634 nA	23.0 ± 0.2 %
PiLas laser @ 40 MHz, tune 93%	~340 nA	23.3 ± 0.3 %
Monochromator	~63 nA	22.9 ± 0.1 %

Table 2
HRPPD QE measurement results. Only statistical errors quoted.

One can see that the measured values show a certain trend in the laser data, namely the QE estimate goes up with decreasing HRPPD photocathode current. However, the monochromator point (continuous wave beam, but also low intensity) is not really consistent with this observation.

We should also mention that a Hamamatsu calibration coefficient came out slightly different for the monochromator case, as compared to the laser light source, which fact we tentatively attribute to a usage of a pellicle beam splitter and a possible small residual polarization of the laser light after coupling into the multimode fiber (while the monochromator light is expected to be unpolarized). For the purposes of this report, we are therefore taking a QE value of 24.3 ± 0.1 (stat) %, obtained with a PiLas laser at the lowest intensity presented in Table 2, with the understanding that this number may have a substantial systematic uncertainty up to at least ± 0.5 % associated with it.

6 HRPPD Collection Efficiency

The Collection Efficiency follows from the PDE and QE measurements at the same wavelength and at the same physical location in the HRPPD active area as CE = PDE/QE. Substituting the numbers obtained in the last two sections, one can see that the HRPPD CE is about 79 %. This number looks reasonable given that most of the primary photoelectrons hitting the interstitial space between the pores of the top surface of the first MCP either do not bounce back or do not make it into the pores with an energy sufficient to initiate an avalanche. For the MCPs used in EIC HRPPDs, the pores occupy about 70 % of the surface area, in a reasonable agreement with our CE estimate.

The proposed technique also allows one to use timing information on event per event basis in order to disentangle contributions of "prompt" photoelectrons and those which bounced off the interstitial space and initiated the avalanche with a delay of up to several hundred picoseconds. The fraction of events in the core out of the total signal events is measured to be approximately 97.5%.

References

Lehmann, A. et al. (2024). “Systematic approach to measure the performance of microchannel-plate photomultipliers”. In: *Nuclear Instruments and Methods in Physics Research Section A: Accelerators, Spectrometers, Detectors and Associated Equipment* 1065, p. 169536. ISSN: 0168-9002. DOI: https://doi.org/10.1016/j.nima.2024.169536. URL: https://www.sciencedirect.com/science/article/pii/S0168900224004625.